Dry Chamber Wall Thermo-Mechanical Behavior and Lifetime under IFE Cyclic Energy Deposition

A. R. Raffray, D. Haynes[1], R. R. Peterson[1], M. S. Tillack, X. Wang, M. Zaghloul

University of California, San Diego, 460 EBU-II, La Jolla, CA 92093-0417, USA
[1]University of Wisconsin, Fusion Technology Institute, 1500 Engineering Drive, Madison, WI 53706-1687, USA

This paper presents results from analyses of dry wall thermo-mechanical behavior based on recent photon and ion spectra for direct drive and indirect drive targets. Implication of the results on chamber lifetime is discussed and some key issues summarized.

1. Introduction

Lifetime is a key issue for the IFE dry chamber wall configuration. Past studies, such as SOMBRERO [1], indicated the need for a protective gas at a significant pressure (e.g. Xe at ~0.5 torr) to prevent unacceptable wall erosion for a carbon chamber wall even for direct-drive targets. This creates a formidable challenge for such a design since the presence of a gas would have to also accommodate target and laser requirements. Recent studies indicated that only minimal target temperature increase (~1 K) can be tolerated during injection to maintain the required target uniformity for a symmetrical burn. High speed target injection (~100's m/s) through a background gas could result in higher target temperature deviation due to convection and friction effects [2]. The presence of a background gas could also lead to laser breakdown depending on the gas density [1]. Until recently, no reasonable design window seemed to exist satisfying the conflicting chamber gas constraints from wall protection on one hand and from the latest target and laser considerations on the other.

A recent effort as part of the ARIES-IFE program has provided a more detailed assessment of dry chamber wall based on ion and photon spectra from a new direct-drive (DD) target (with a yield of 154 MJ, including 2.14 MJ from x-rays, 18.1 MJ from fast ions from the thermonuclear burn, and 24.9 MJ from debris ion kinetic energy) proposed by NRL[3,4], and an updated indirect-drive (ID) target (with a yield of 458 MJ, including 115 MJ from x-rays, 8.43 MJ from fast ions and 18.1 MJ from debris ions) from LLNL[4,5]. Several material options were considered including carbon (C) and tungsten (W) flat wall and a high-porosity fibrous C configuration to maximize the incident surface area and help accommodate the energy deposition. Detailed analyses using very fine meshes were performed for both the energy deposition from the photons and ions and the thermal behavior of the wall. For each case analyzed, the chamber wall temperature was calculated as well as the corresponding surface melt layer (for W) and evaporation.

2. Energy Deposition

The energy deposition in the material was calculated based on the photon and ion spectra for the DD and ID targets. A 1-D slab geometry was assumed and the calculations performed for C and W. An attenuation calculation was used for the photon energy deposition based on data for the attenuation coefficient in the material (including photo-electric and Compton scattering effects) as a function of the photon energy [6]. The ion deposition calculation included both the electronic and nuclear stopping powers which were obtained as a function of ion energy from SRIM [7]. The calculation proceeded by following ions at discretized energy levels from the spectra though the material slab. Figure 1 shows an example of the

energy deposition as a function of penetration depth for C and W for the DD spectra assuming a chamber radius of 6.5 m and no protective gas in the chamber.

The calculation procedure included the time of flight spreading of the photon and ion energy deposition. The photons travel much faster than the ions and would reach the chamber wall within about 20 ns in the case without protective gas. The ions take longer to reach the chamber wall. As an example, a simple estimate of the ion time-of-flight based on kinetic energy is shown in Figure 2 for the DD target spectra for a case without any protective chamber gas. The fast ions reach the wall within about 0.2 to 1 μs whereas the slow ions reach the wall within 1 to 2.5 μs.

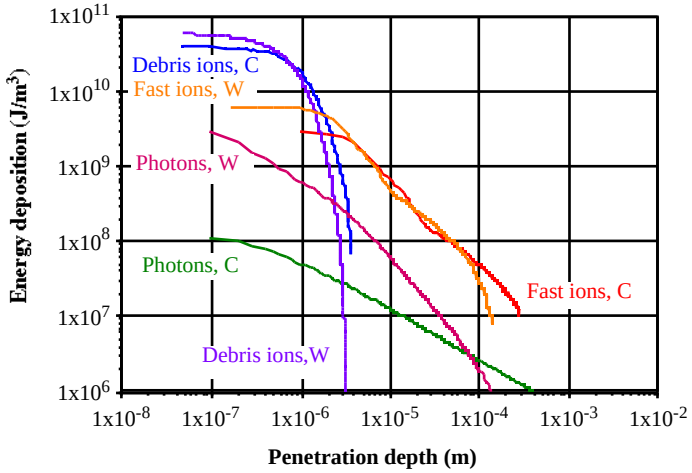

Figure 1 Energy deposition in W and C as a function of penetration depth for DD target x-ray and ion spectra.

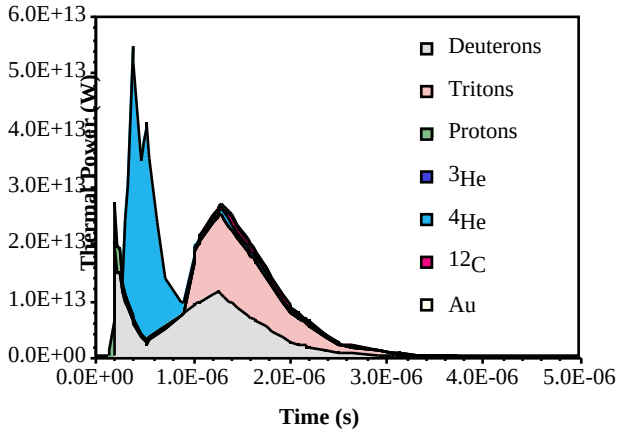

Figure 2 Temporal distribution of ion power at chamber wall for DD target ion spectra.

3. Thermal Analysis

The thermal analysis was carried out using ANSYS with the calculated energy deposition over time as input and using BUCKY an integrated 1-D code calculating the photon and ion energy deposition and the wall thermal response for cases with and without a protective gas [8]. The thermal calculations include the effect of melting in the case of W whereby the phase change latent heat is included when the local temperature reaches the melting point (3410°C for W) and the corresponding melt layer thickness is estimated [9]. Evaporation is included as a function of temperature, increasing exponentially as the evaporation point is reached; the corresponding material loss is also estimated. Temperature-dependent properties were utilized for both C and W; the thermal conductivity of C tends to decrease appreciably with neutron irradiation and the thermal conductivity data for irradiated C (1 dpa) were used [9].

3.1 Direct Drive Target Spectra with No Protective Gas in the Chamber

The calculations were performed for a 3-mm slab, one side subjected to the photon and ion fluxes and the other convectively cooled with an assumed heat transfer coefficient of 10 kW/m^2-K. These analyses for the DD target spectra conservatively assumed no protective gas in the chamber. Table I shows the results for C for two different coolant temperatures. The C sublimation rate per shot and per year assuming an 85% reactor availability are also shown. From these results, a C wall can survive the photon and ion energy deposition from this target even without gas protection with some margin to allow for design optimization on various parameters such as the chamber radius and target yield.

Various concerns exist regarding the use of C as chamber wall armor. In addition to sublimation, several other erosion processes need to be considered including physical and chemical sputtering and radiation-enhanced sublimation [10]. A key concern is the possibility

of tritium trapping by co-deposition with C atoms in colder region such as in penetration lines leading to unacceptably large tritium inventories [10,11]. For this reason, it is prudent to consider other armor material candidates such as refractory metals. Table I also shows the results for a W armor for coolant temperatures, T_{cool}, of 500°C and 800°C, respectively. These results indicate no W melting for the T_{cool}=500°C case and a melt layer of ~0.8μm for the T_{cool}=800°C case. If melting avoidance is a requirement, T_{cool}, chamber size and/or protective gas density would have to be adjusted correspondingly. However, it is not clear whether total melt avoidance would be required as this would depend on the stability of the melt layer and on the material form and integrity following resolidification. Also of concern are the large temperature gradients at the surface giving rise to stresses that could result in macroscopic erosion (this would apply to any armor), and the He implantation in particular in armor with poor He transport (such as W). The trapped He would accumulate and create defective regions which could result in expulsion of chunks of armor. R&D effort is needed in this area to better understand the problem and to find solutions such as the possible use of porous nanostructure to minimize the characteristic transport length of He in the armor and enable the He to find an open channel and migrate back to the chamber.

Table I Summary of Analysis Results for C and W Flat Wall with No Protective Gas for DD Target Spectra

Armor	Cool. Temp. T_{cool} (°C)	Max. Armor Temp. T_{max} (°C)	C Subl. Loss per shot/ W melt layer (μm)	C Subl. Loss per Year (μ m)
C	500	1955	$5x10^{-11}$	~0.01
C	800	2220	$4x10^{-9}$	~1
W	500	3237	0	N/A
W	800	3570	~0.8	N/A

Table II Summary of Analysis Results for C Fibrous Surface with No Protective Gas for RHEPP Ion Spectra [9]

Porosity	Fiber Diameter. (μm)	Incidence Angle (°)	T_{max} at Fiber Tip (°C)
0.98	29.6	5	4098
0.98	29.6	10	4031
0.98	29.6	20	3949
0 (Flat Wall)	N/A	N/A	4130

An engineered surface increasing the incident surface area was considered to improve energy deposition accommodation. Figure 3 shows an example of such a surface. It consists of a high porosity C fiber carpet which could be coated with W. A model was developed for the energy deposition and the thermal analysis based on a single fiber unit cell [9] and results indicated substantially less erosion than for a flat case. This has been confirmed by recent experimental results from RHEPP showing virtually no erosion from the fibers and significant erosion for a comparable C flat case under an ion fluence of about 5 J/cm^2[13,9]. Modeling results based on the RHEPP ion spectra are summarized in Table II for different assumed angles of incidence. The incident area increases with incidence angle resulting in somewhat lower T_{max} and sublimation at the fiber tip than for the flat wall case. In addition, the very low density of the fiber configuration (~2%) results in a correspondingly smaller overall erosion.

3.2 Indirect Drive Target Spectra with Protective Gas in the Chamber

The threat spectrum produced by ID targets differs significantly from that of DD targets. The massive hohlraum converts capsule ion and x-ray debris into relatively soft and more potentially damaging x-rays. In order for the chamber dry wall armor to survive, some buffer gas must be present to absorb the prompt x-rays, re-radiating their energy over a longer period of time. To determine the minimum amount of Xe necessary to prevent significant first wall vaporization (assumed for these calculations as more than one monolayer of graphite per shot) a series of BUCKY[8] radiative hydrodynamic simulations were conducted. An example of

the results is illustrated in Figure 4 which shows the minimum Xe pressure as a function of the pre-shot armor temperature. The curve in this figure indicates that, for pre-shot armor temperatures < 1000°C, the amount of Xe necessary to protect such a chamber wall is significantly less than the 0.5 torr previously estimated in the SOMBRERO study. Unlike the DD laser case, the presence of Xe actually aids in some heavy ion driver beam transport mechanisms, and target heating and injection complications from the presence of the Xe gas are much less important for the massive hohlraum-protected ID target than for the bare cryogenic DD laser target.

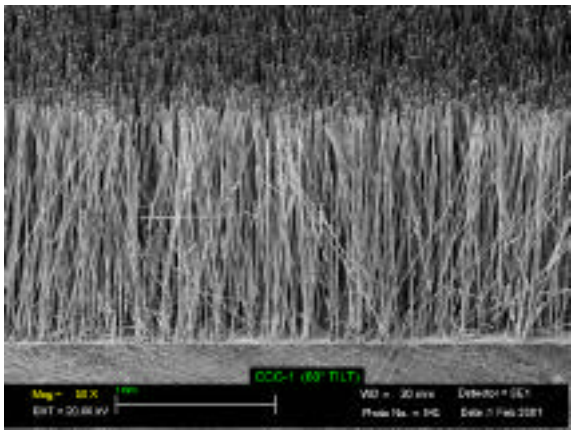

Figure 3 Carbon fibrous carpet from Energy Science Laboratories Inc. San Diego [12].

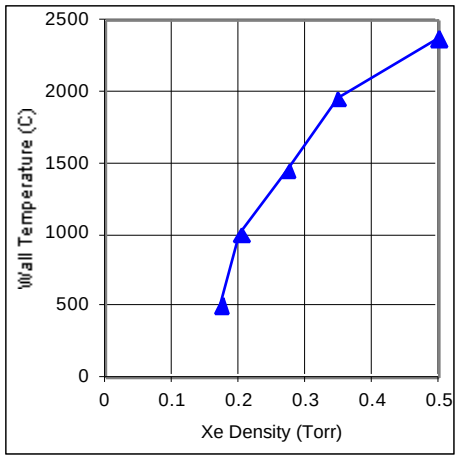

Figure 4 Pre-shot T_{wall} at which one C monolayer is vaporized per shot as a function of Xe density for a 6.5 m radius chamber under the ID target spectra.

4. Summary

Encouraging results were obtained from IFE dry wall analyses based on recent DD and ID target spectra. The analysis included the key effect of photon and ion time of flight on the energy deposition and showed that for the direct drive target, a design window exist even for a case without a protective gas which will greatly help to accommodate target thermal control and laser breakdown requirements. The presence of a protective gas such as xenon is much more important for the ID spectra but at a much lower pressure than previously considered.

References

[1] W. R. Meier, et al., OSIRIS and SOMBRERO Inertial Fusion Power Plant Designs: Final Report, WJSA-92-01 (DOE/ER/54100-1), March 1992.

[2] D. T. Goodin et al., Nuclear Fusion 41 (5) May 2001.

[3] S. E. Bodner, et al., Physics of Plasmas 7(6), June 2000, pp. 2298-2301.

[4] http://aries.ucsd.edu/ARIES/WDOCS/ARIES-IFE/SPECTRA/

[5] D. A. Callahan-Miller and M. Tabak, Nuclear Fusion, Vol. 39, No. 7, July 1999.

[6] http://aries.ucsd.edu/LIB/PROPS/PHOTON/

[7] http://www.srim.org/

[9] A. R. Raffray, R. R. Peterson, et al., Assessment of IFE dry chamber walls, to appear in Fusion Engin. & Design.

[8] J.J. MacFarlane, G.A. Moses, R.R. Peterson, UWFDM-984, Univ. of Wisconsin, 1995.

[10] J. Roth, et al., Erosion of graphite due to particle impact," Nuclear Fusion, 1991.

[11] http://aries.ucsd.edu/LIB/MEETINGS/0103-ARIES-TTM/

[12] http://www.esli.com

[13] T. Renk, http://aries.ucsd.edu/HAPL/MEETINGS/0111-HAPL/program.html